

Platinum group elements and gold in ferromanganese crusts from Afanasiy–Nikitin seamount, equatorial Indian Ocean: Sources and fractionation

V K BANAKAR^{1,*}, J R HEIN², R P RAJANI¹ and A R CHODANKAR¹

¹*National Institute of Oceanography, Dona Paula, Goa 403 004, India.*

²*U.S. Geological Survey, MS999, Menlo Park, California, USA.*

**e-mail: banakar@nio.org*

The major element relationships in ferromanganese (Fe–Mn) crusts from Afanasiy–Nikitin seamount (ANS), eastern equatorial Indian Ocean, appear to be atypical. High positive correlations ($r = 0.99$) between Mn/Co and Fe/Co ratios, and lack of correlation of those ratios with Co, Ce, and Ce/Co, indicate that the ANS Fe–Mn crusts are distinct from Pacific seamount Fe–Mn crusts, and reflect region-specific chemical characteristics. The platinum group elements (PGE: Ir, Ru, Rh, Pt, and Pd) and Au in ANS Fe–Mn crusts are derived from seawater and are mainly of terrestrial origin, with a minor cosmogenic component. The Ru/Rh (0.5–2) and Pt/Ru ratios (7–28) are closely comparable to ratios in continental basalts, whereas Pd/Ir ratios exhibit values (< 2) similar to CI-chondrite (~ 1). The chondrite-normalized PGE patterns are similar to those of igneous rocks, except that Pd is relatively depleted. The water depth of Fe–Mn crust formation appears to have a first-order control on both major element and PGE enrichments. These relationships are defined statistically by significant ($r > 0.75$) correlations between water depth and Mn/Co, Fe/Co, Ce/Co, Co, and the PGEs. Fractionation of the PGE–Au from seawater during colloidal precipitation of the major-oxide phases is indicated by well-defined linear positive correlations ($r > 0.8$) of Co and Ce with Ir, Ru, Rh, and Pt; Au/Co with Mn/Co; and by weak or no correlations of Pd with water depth, Co-normalized major-element ratios, and with the other PGE ($r < 0.5$). The strong enrichment of Pt (up to 1 ppm) relative to the other PGE and its positive correlations with Ce and Co demonstrate a common link for the high concentrations of all three elements, which likely involves an oxidation reaction on the Mn-oxide and Fe-oxyhydroxide surfaces. The documented fractionation of PGE–Au and their positive association with redox sensitive Co and Ce may have applications in reconstructing past-ocean redox conditions and water masses.

1. Introduction

Central Pacific seamount ferromanganese crusts (Fe–Mn crust) enrich Co up to 2% and Pt up to 3 ppm (Halbach *et al* 1989a and b; Usui and Someya 1997). In addition to Pt, the other PGE (Ru, Rh, Ir, and Pd) as well as Au are enriched many-fold compared to their concentrations in seawater from which the Fe–Mn crusts precipitated

(Hein *et al* 2000; Palmer and Turekian 1986). Hein *et al* (2000) showed that Pt, Rh, and Ir are derived from seawater, whereas Pd is hosted mostly in detrital minerals, which are intimately mixed with Fe–Mn oxide minerals in Fe–Mn crust. Although PGE is a group of coherent siderophile metals, they generally do not exhibit good coherency in many marine systems because of their fractionation by several oceanographic and geochemical processes

Keywords. Indian Ocean; ferromanganese crusts; platinum group elements; source and fractionation.

such as their efficiency of formation of complexes and adsorption to host phases under variable redox conditions in ambient water (Sawlowicz 1993; Hodge *et al* 1985).

The PGE gained importance after the discovery of Ir anomaly associated with the Cretaceous-Tertiary (KT) boundary mass-extinction that resulted from a catastrophic bolide impact (Alvarez *et al* 1980). Subsequently, studies exploring the potential use of PGE as indicators of large-scale alteration of Earth's atmosphere, and in turn of ecosystems, have been discussed based on continental and marine sedimentary sequences across the KT boundary (e.g., Lee *et al* 2003). Anomalous PGE concentrations in several sedimentary deposits, however, are not associated with global mass extinction and alternative mechanisms, such as volcanic input, diagenesis, authigenic precipitation from seawater, among others, have been proposed (e.g., see Colodner *et al* 1992; Strong *et al* 1987). The PGE chemistry of seawater can be better understood from studying hydrogenetically precipitated Co-enriched Fe–Mn crusts deposited on open-ocean seamounts where diagenetic and hydrothermal metal inputs are uncommon. However, PGE studies of marine hydrogenetic and authigenic deposits are few.

Previous studies of PGE in Fe–Mn crusts mostly focused on the mechanism of Pt enrichment (*see* Halbach *et al* 1989a, 1989b) because Pt adds to the potential economic value of the deposits (Hein *et al* 2000). Here, we present the first PGE and Au data for Fe–Mn crusts occurring on ANS and discuss aspects related to their fractionation and dominant sources. The ANS is thought to have formed during the Late Cretaceous (Sborshchikov *et al* 1995) and shows convincing evidence of subaerial weathering followed by submergence (Banakar *et al* 1997). The ANS attained its present configuration around Late Miocene as indicated by the continuous growth of Fe–Mn crusts over conglomeritic substrate rocks containing rounded basalt clasts and brachiopod casts embedded in neomorphic carbonate cement (Banakar *et al* 1997). The Fe–Mn crusts from this seamount show Co and Ce enrichments up to 0.9% and 0.4%, respectively (Rajani *et al* 2005). Because Fe–Mn crust composition changes in response to long-term variations in oceanographic conditions and continental erosion (*see* Banakar and Hein 2000; Banakar *et al* 2003 and references therein), the present study provides useful clues for understanding PGE anomalies in the marine environment. However, the relative importance of each mechanism is difficult to quantify using bulk Fe–Mn crust (*i.e.*, total Fe–Mn oxide layer excluding substrate rock) PGE dataset.

2. Material and methods

Fe–Mn crusts were recovered by dredging along short tracks of ~ 100 m on the slopes of ANS during two cruises of the R. V. *A A Sidorenko* (AAS-59 and AAS-65: February and August 2003 respectively), undertaken for exploration of Co-enriched seamount Fe–Mn crusts in the EEIO. Most ANS volcanic peaks hosting Fe–Mn crusts rise from a large plateau at ~ 3.2 km water depth that extends ~ 400 km north–south and ~ 250 km east–west at $\sim 3^\circ$ S latitude and $\sim 83^\circ$ E longitude (figure 1). The base of the ANS is at ~ 4.5 km water depth. The thickness of Fe–Mn oxide layer varies from a coating to ~ 7 cm. Fe–Mn crusts were collected from water depths ranging from 1.6 km (top of the highest peak) to 3.2 km (top of the plateau). Fe–Mn crusts were not recovered from 3.2 km (top of the plateau) to 4.5 km (base of the seamount or surrounding seafloor). Carbonate sedimentation on plateau and lower flanks of the seamount may be the reason for absence of Fe–Mn crusts here. Thus sedimentation may have prevented the growth of Fe–Mn crusts on plateau and basal slopes. We recovered samples of Fe–Mn crusts in over 25 dredge hauls from different depths and selected nine representative samples for this study, for which Mn, Fe, Co, Ce, PGE, and Au data were obtained. Only those Fe–Mn crust samples having a > 2 cm-thick oxide layer with Mn and Fe contents each $> 14\%$ were used in order to limit this study to samples with minimum dilution by non-hydrogenetic components, such as carbonate and silicate detritus.

The Fe–Mn oxide layer was chipped off the substrate rocks and ground to fine powder (-200 mesh). Powdered samples were oven dried at $\sim 110^\circ$ C overnight and aliquots were used for the various measurements. The Fe, Mn, Co, and Ce concentrations were measured on 6N HCl leachates using a Perkin–Elmer[®] OPTIMA-2000 DV ICP-OES. PGE and Au were measured by both Ni- and Pb-fire assay with an ICP-MS finish at the U.S. Geological Survey (Baedecker 1987). For Ni-sulfide, the sample powder (~ 15 g) was mixed with a flux prepared from soda ash, borax, silica, sulfur, and nickel carbonate and fused at 1200° C. During fusion, Ni, PGE, and Au sulfides were formed. The fused mixture was treated with HCl in which the Ni sulfide was dissolved and removed. The remainder, containing PGE and Au, was dissolved in aquaregia in a borosilicate test tube and diluted with nitric acid to the required volume for measurement. A control blank was run before and after the sample run and each blank value was below the detection limits of 5 ppb for Au; 2 ppb for Ir, Os, Pd, Pt, and Ru; and 1 ppb for Rh. Repeat analysis of reference standards SRM7b yielded,

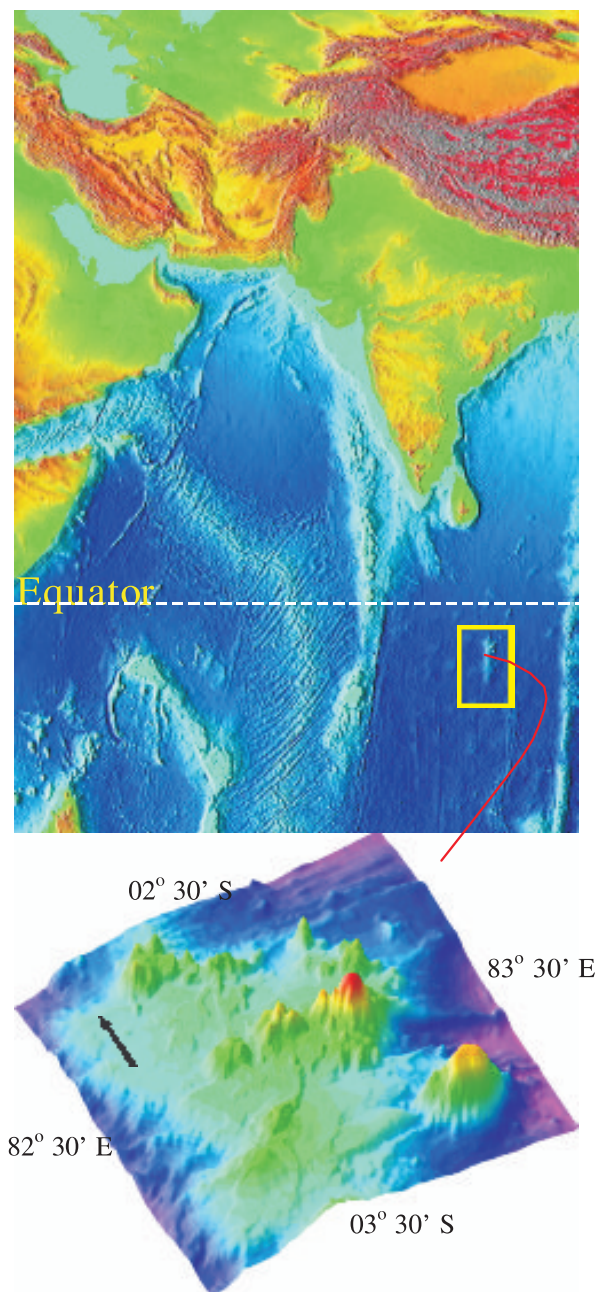


Figure 1. Location of the Afanasiy–Nikitin seamount (enclosed by box) in the Indian Ocean (www.ngdc.noaa). Location details are given in the text. The lower panel is vertically exaggerated 3-D colour coded multibeam swath-bathymetric map of northern part of the seamount (100×100 km) generated on board R. V. *Boris Petrov* in March 2005. The samples are from two transects (approximately east–west and north–south) across the central cluster of mounts. Pink colour indicates deepest (> 4500 m) region and red colour indicates shallowest (< 1700 m) region. Arrow on the lower panel indicates north specific only to the lower panel.

Ir 85 ppb, Os 59 ppb, Pd 1352 ppb, Pt 3617 ppb, Rh 224 ppb, Ru 424 ppb and Au 271 ppb as against the Mintek certified values of 90 ppb, 63 ppb, 1540 ppb, 3740 ppb, 240 ppb, 460 ppb and 270 ppb

respectively. Thus the accuracy of the data presented here is better than $\pm 10\%$. Analytical precision was better than 20% for Au, Ir, and Pd, 10% for Rh, and 5% for Ru and Pt. Os was less than its detection limit (2 ppb) for all but one sample (ADR 27), which has 4 ppb. Ag was measured by atomic absorption spectrometry, but concentrations were less than the detection limit of 1 ppm in all samples. Hence, Os and Ag will not be discussed further. As the Au concentration in Fe–Mn crusts never falls to zero, we multiplied its concentration at detection limit (5 ppb) by 0.5 for statistical analysis. The PGE in few duplicate samples were also measured at the ICP–MS facility of National Geophysical Research Institute, India, following the same procedures of sample preparation (see Balaram *et al* 2005), and the results from both the laboratories are comparable within $\pm 10\%$ for high concentration PGE (Pt, Ru, Rh) and within $\pm 20\%$ for low concentration PGE (Pd, Ir) and Au.

3. Results and discussion

The dominant elements in ANS Fe–Mn crusts, Mn and Fe, vary between 14% and 25%, followed by Co (0.35% to 0.85%) and Ce (0.09% to 0.24%) (table 1). Data for Si, Al, and Ti are not available. However, those elements typically occur in concentrations higher than Co and Ce as they are mostly associated with silicate detritus, which is the second abundant component after Fe–Mn oxide. However, Ti can have a significant hydrogenetic component (Koschinsky and Halbach 1995). The generally observed correlation of Co with Mn and Ce with Fe in seamount Fe–Mn crusts (e.g., Banakar and Hein 2000; De Carlo and McMurtry 1992; Halbach *et al* 1989b; Hein *et al* 2000; Koschinsky and Hein 2003) does not occur in the ANS Fe–Mn crust data set (table 2). Such correlations led Rajani *et al* (2005) to hypothesize the independent precipitation of Co and Ce oxides. This hypothesis needs to be tested by EXAFS or XANES analyses of the oxide phases. We discuss this possibility in a later section by examining correlations obtained from Co-normalized element ratios. Elements are normalized to Co because it has a nearly constant flux from seawater and is almost solely of hydrogenetic origin.

The subequal amounts of Fe and Mn (Mn/Fe 0.94–1.27) in the ANS Fe–Mn crusts indicate a hydrogenetic origin and an absence of hydrothermal input (Hein *et al* 2000; Banakar *et al* 1997). Therefore, PGE-enrichment processes from hydrothermal activity (Halbach *et al* 1989b; Koide *et al* 1991; Officer and Drake 1985) may not have contributed to the PGE and Au concentrations of ANS Fe–Mn crusts. Substrate rocks neither

Table 1. Major element, PGE–Au and cobalt normalized element ratio of Afanasiy–Nikitin seamount Fe–Mn crusts compared with potential source material.

Sample code	Depth	Mn*	Fe*	Co*	Ce*	Ir**	Ru**	Rh**
CC1/DR25	1.75	15.5(20)	16.0(21)	0.77	0.29(0.4)	14(1.8)	31(4.0)	48(6.2)
CC1/DR12B	1.91	18.0(24)	14.2(19)	0.75	0.26(0.3)	08(1.1)	24(3.2)	24(3.2)
CC2/ADR19	2.00	22.0(30)	19.3(26)	0.74	0.24(0.3)	09(1.2)	20(2.7)	38(5.1)
CC2/ADR27	2.06	24.9(29)	24.2(28)	0.85	0.19(0.2)	10(1.2)	31(3.6)	23(2.7)
CC2/ADR26	2.10	19.6(47)	19.2(46)	0.42	0.09(0.2)	03(0.7)	12(2.9)	06(1.4)
CC2/ADR11	2.20	18.7(32)	19.5(33)	0.59	0.13(0.2)	06(1.0)	17(2.9)	13(2.2)
CC2/ADR10	2.62	18.1(33)	19.2(35)	0.55	0.12(0.2)	06(1.1)	17(3.1)	13(2.4)
CC2/ADR4	3.15	20.9(47)	20.2(46)	0.44	0.14(0.3)	05(1.1)	15(3.4)	10(2.3)
CC2/ADR24	3.20	22.2(63)	22.6(65)	0.35	0.13(0.4)	04(1.1)	12(3.4)	07(2.0)
CI Chondrite (Anders and Ebihara 1982)						473	714	134
Iron meteorite (Crocket 1972)						4	73	na
Karoo basalt (Naldrett 1981)						88	147	80
Duluth basalt (Naldrett 1981)						6	15	16
Deccan basalt (Crocket and Paul 2004)						0.024	na	na
Carbonate ooze (Hodge et al 1985)						na	na	na
Siliceous ooze (Hodge et al 1985)						na	na	na
Ultramafic rocks (Crocket 1981)						3.8	6.1	3
Black shale-Chine (Coveney et al 1992)						0.1	16	na
Continental crust (Govett 1983)						1	na	1
MORB-Pacific (Peucker-Ehrenbrink et al 2003)						0.01	na	na
MORB-Atlantic (Peucker-Ehrenbrink et al 2003)						0.03	0.7	na

Depth in km; * – wt. %; ** – ppb; Values in parentheses are Element/Cobalt ratio ($\times 10^b$); na – not available. All values are rounded to nearest decimal. All Ag and Os concentrations are below detection limit.

§ – estimated values (see text).

provide fluids that contribute to the formation of Fe–Mn crusts nor diagenetically influence their composition (Banakar and Hein 2000; Hein and Morgan 1999).

The sources of PGE and Au in seawater are terrestrial and cosmogenic inputs and these elements occur in both dissolved and particulate forms (Halbach et al 1989a; Hein et al 2005). The detrital component in seamount Fe–Mn crusts is largely derived from erosion of continental crust and from input of local volcanogenic minerals. Average continental crust contains very low PGE–Au concentrations (Kyte and Wasson 1986). Most of the silicate detritus reaching the ANS region is derived from Himalayan erosion with insignificant contributions from peninsular Indian basalts, hence detrital input cannot be the dominant host for noble metals in these Fe–Mn crusts. Therefore, the PGE in these Fe–Mn crusts must be considered as having been derived predominantly from seawater.

3.1 Sources for and incorporation of PGE–Au in Fe–Mn crusts

The PGE contents in seawater are extremely low: Ir, ~ 0.0013 ppt (Hodge et al 1986); Ru, ~ 0.002 ppt (Goldberg 1987); Rh, ~ 0.09 ppt

(Bertine et al 1993); Pt, 0.2 to 1 ppt (Goldberg et al 1986; Turretta et al 2003), and Pd, ~ 0.04 ppt (Goldberg 1987). Their enrichment in the ANS Fe–Mn crusts over seawater values is about 10^4 to 10^7 times. However, this enrichment is 2–3 orders of magnitude lower than the enrichment of the most dominant elements, such as transition and rare earth elements (see Hein et al 2003, 2005). On a global scale, the PGE are fractionated twice, once during weathering and transfer to seawater, where the order of decreasing abundance changes from Pt–Pd–Ru–Rh–Ir to Pt–Rh–Pd–Ru–Ir; and a second time during incorporation from seawater into Fe–Mn crusts where the order of abundance then changes to Pt–Ru–Rh–Ir–Pd (Hein et al 2005).

The uptake of PGE and Au in Fe–Mn crusts is not fully understood and the pathways of PGE and Au in marine biogeochemical processes are still largely unknown. Halbach et al (1989a, 1989b) proposed co-precipitation of Pt with Mn oxide due to coupled redox reactions in addition to input of cosmic dust as the causes of Pt enrichment in Pacific seamount Fe–Mn crusts. Hein et al (2003) suggested that Pt is sorbed and then oxidized on the surface of the FeOOH phase, similar to the mechanism that may strongly enrich Te in Fe–Mn crusts. Vonderhaar et al (2000) suggested that Pt

Table 1. (Continued)

Pt**	Pd**	Au**	Pt/Pd	Ru/Rh	Pd/Ir	Pt/Ir	Pd/Ru	Pt/Ru	Pt/Au
780(101)	04(0.5)	2.5(0.3) [§]	195	0.65	0.29	55.7	0.13	25.2	312
357(48)	03(0.4)	2.5(0.3) [§]	119	1.00	0.38	44.6	0.13	14.9	143
568(77)	08(1.1)	13(1.8)	71	0.53	0.89	63.1	0.40	28.4	43.7
286(34)	20(2.3)	18(2.1)	14	1.35	2.00	28.6	0.65	9.2	15.9
102(24)	06(1.4)	15(3.6)	17	2.00	2.00	34.0	0.50	8.5	6.8
166(28)	06(1.0)	11(1.9)	28	1.31	1.00	27.7	0.35	9.8	15.1
149(27)	05(0.9)	07(1.3)	30	1.31	0.83	24.8	0.29	8.8	21.3
111(25)	08(1.8)	13(2.9)	14	1.50	1.60	22.2	0.53	7.4	8.5
101(29)	04(1.1)	19(5.4)	25	1.71	1.00	25.3	0.33	8.4	5.3
953	557	145	1.71	5.33	1.18	2	0.78	1.3	6.6
9.4	4.5	1.3	2.09		1.13	2.4	0.62	1.3	7.2
1330	708	397	1.88	1.84	8.05	15.1	4.8	9	3.4
333	1113	147	0.3	0.94	186	55.5	74.2	22.2	2.3
4.2	13	4.3	0.3		554	175			1.0
3	1.6	na	1.88						
2.3	3.6	na	0.64						
9.1	6.7	na	1.36	2.03	1.76	2.4	1.1	1.5	
15	37	48	0.41		370	150	2.31	0.9	0.3
5	10	4	0.5		10	5			1.3
0.3	0.27	na	1.11		27	30			
0.8	2	na	0.4		67	27	2.86	1.1	

enrichment is closely tied to the diagenetic formation of carbonate fluorapatite in central Pacific Fe–Mn crusts. Diverse mechanisms of PGE enrichment in marine sediments have also been suggested, ranging from microbial activity to cosmic dust (*see* Sawlowcz 1993).

Compared to CI-Chondrites (Anders and Ebihara 1982), ANS Fe–Mn crusts are depleted in PGE–Au, but are significantly enriched compared to pelagic sediment (Esser and Turekian 1988) (table 1). Although the average continental crust is highly depleted in PGE–Au (Crocket and Kuo 1979), continental basalts show considerable enrichments (Crocket 1981; Crocket and Paul 2004; Naldrett 1981), nearly of the magnitude found in ANS Fe–Mn crusts (table 1). However, PGE variations in different basalts are large, as evident from the Karoo, Duluth, and Deccan basalts (table 1). Nevertheless, cosmogenic debris and plateau basaltic rocks (large igneous complexes) may be important sources of seawater PGE–Au.

Chondrite-normalized PGE patterns of ANS Fe–Mn crusts are closely comparable for the entire water-depth range (figure 2). They demonstrate the consistent Pt enrichment over other PGEs. The anomalous enrichment of Pt over Pd in marine Fe–Mn nodules and crusts (Pt/Pd, 50–1000) compared to seawater ratios (~ 4 –5) was recognized by

Hodge *et al* (1985). They proposed oxidation of Pt from the dissolved pool, similar to Ce and Co, to explain its several orders of magnitude enrichment in Fe–Mn nodules and crusts. The PGE patterns from Ir to Pt in ANS Fe–Mn crusts are similar to their fractionation patterns in terrestrial magmas, which exhibit fractionation in the order of decreasing melting points (Barnes *et al* 1985). This observation is of interest because the lowest melting point is for Pd, which apparently fractionates last during magmatic crystallization (Barnes *et al* 1985), but shows depletion relative to the other chondrite-normalized PGE in ANS Fe–Mn crusts. This anomalous depletion of Pd suggests that it was decoupled from the other PGE at the source before reaching the oceanic reservoir, if continental crust was their main source. Further, if the oceanic reservoir of PGE is the result of weathering input from continental rocks, then their relative abundances should reflect their mobility during low temperature chemical weathering, which would also follow igneous fractionation trend. The lower melting point PGE (e.g., Pd) is fractionated from the igneous rock more readily than the higher melting point PGE (e.g., Ru). This weathering fractionation pattern may be overprinted if there are other significant sources not governed by magmatic crystallization, such as the weathering of PGE-rich

Table 2. Correlation coefficients of water depth, major elements and PGE–Au in Afanasiy–Nikitin seamount Fe–Mn crusts.

Depth	Mn (Mn/Co)	Fe (Fe/Co)	Co	Ce (Ce/Co)	Ir (Ir/Co)	Ru (Ru/Co)	Rh (Rh/Co)	Pt (Pt/Co)	Pd (Pd/Co)	Au (Au/Co)
1.0										
Mn (Mn/Co)	1.0									
Fe (Fe/Co)	0.8 (1.0)	1.0								
Co	*0.02	*0.24	1.0							
Ce (Ce/Co)	*0.3(0.0)	*0.5(0.0)	0.79	1.0						
Ir (Ir/Co)	*0.7(*0.2)	*0.3(*0.4)	0.86	0.9(0.6)	1.0					
Ru (Ru/Co)	*0.7(0.0)	*0.2(*0.1)	0.92	0.8(0.5)	0.9(0.7)	1.0				
Rh (Rh/Co)	*0.7(*0.6)	*0.4(*0.7)	0.79	0.9(0.6)	0.9(0.9)	0.8(0.4)	1.0			
Pt (Pt/Co)	*0.7(*0.6)	*0.5(*0.6)	0.73	0.9(0.6)	0.9(0.8)	0.7(0.4)	1.0(1.0)	1.0		
Pd (Pd/Co)	*0.1(0.3)	0.7(0.3)	0.43	0.0(*0.5)	0.2(*0.3)	0.4(0.1)	0.0(*0.4)	*0.1(*0.5)	1.0	
Au (Au/Co)	0.5(0.7)	0.9(1.0)	*0.41	*0.6(*0.0)	*0.5(*0.5)	*0.4(*0.1)	*0.5(*0.6)	*0.5(*0.6)	0.5(0.5)	1.0

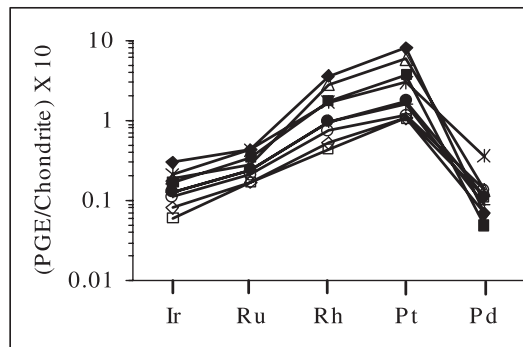
* = Negative coefficients; $R > 0.6$ is significant at 95% confidence level.

Figure 2. CI Chondrite-normalized PGE patterns of the Afanasiy–Nikitin seamount Fe–Mn crusts.

black shales or if the dominant source of Pd in seawater was cosmogenic debris.

To precisely define the sources, we examined the ratios of different PGE in ANS Fe–Mn crusts and compared them with those of probable source materials. Further, we assessed PGE–Au fractionation and acquisition by evaluating their relationship with dominant mineral phases in the ANS Fe–Mn crusts and their water depths. The depletion of Pd documented in the chondrite-normalized PGE patterns of ANS Fe–Mn crusts (figure 2) can be explained by the Pd/Ir ratios, which are similar to that of CI-chondrites (~ 1), but deviate significantly from those in continental and oceanic crust (table 1). This suggests that the source of Pd and Ir could be largely extraterrestrial. The other PGE ratios in ANS Fe–Mn crusts such as Ru/Rh, Pt/Ir, and Pt/Ru closely resemble plateau basalt ratios and are distinctly different from ratios in meteoritic and black-shale. The Pt/Au ratios on the other hand are difficult to assess because they show both igneous and cosmogenic signals in different samples. These various PGE ratios demonstrate that the Ir and Pd in ANS Fe–Mn crusts are derived from the ambient seawater but originated largely from a cosmogenic source, whereas Ru, Rh, and Pt in seawater and the Fe–Mn crusts appear to have been derived from chemical weathering of continental crust and plateau basalts.

Hydrothermal sources of PGE to seawater are poorly known and hence difficult to evaluate as a source for Fe–Mn crusts. Mid-ocean ridge basalt generally has low PGE concentrations (table 1) and is therefore not a likely source for these elements. However, ultramafic rocks (such as peridotite, serpentinite, etc. associated with transform faults and ridge intersections) leached by circulating fluids along spreading centers may have higher PGE concentrations and may act as local sources.

The Pt/Pd ratios of pelagic sediments (~ 5 : Esser and Turekian 1988; Hodge *et al* 1985) are

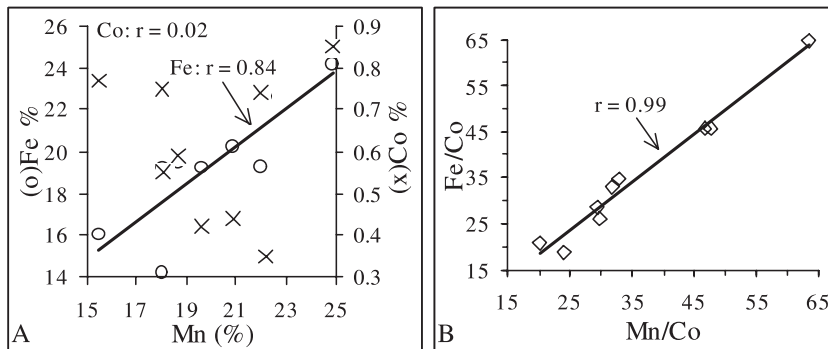


Figure 3. Fe and Mn relationship in the Afanasiy–Nikitin seamount Fe–Mn crusts (A) showing significant improvement in association after normalizing with Co (B). The positive correlation between Fe and Mn and lack of correlation between Mn and Co are atypical of crusts studied elsewhere.

similar to the mean seawater ratio of ~ 4.5 (Hodge *et al* 1985). In contrast, ANS Fe–Mn crusts and other ocean Fe–Mn deposits show significantly higher Pt/Pd ratios (≥ 100) than do pelagic sediments. These ratios suggest high efficiency for Pt acquisition by marine Fe–Mn deposits compared to pelagic sediments, which are affected by diagenetic processes.

3.2 Major element-phases and water-depth associations

We obtained best fits for scatter plots of major elements and PGE–Au data to understand how PGE and Au are fractionated in the ANS Fe–Mn crusts. Several oceanographic and geochemical processes dictate the composition of Fe–Mn crusts (Frank *et al* 1999), where water depth being an important parameter. Therefore, more fundamental chemical associations between various components of the crusts can be determined by eliminating the effects of water depth, accretion rate, and temporal changes in seawater chemistry. Normalizing the chemical data to an element that has a constant flux in space and time to the Fe–Mn crusts can approximate that ideal condition. The flux of Co to Fe–Mn crusts is thought to be constant ($2.9 \mu\text{g}/\text{cm}^2 \cdot \text{ka}$) at all water depths over large time-spans, of several millions of years, as determined for Pacific seamount Fe–Mn crusts (Halbach *et al* 1983). Hence, Co-normalized element ratios may provide a better understanding of the chemical associations between the elements than those obtained from element concentration data. Both linear and non-linear relationships between major components and PGE–Au are evident (table 2 and figures 3–5), which demonstrate that the element enrichment processes are complex in Fe–Mn crusts. We looked for coherence in data distribution in the scatter plots and calculated r -values of the linear best-fits obtained for concentration and

Co-normalized data (table 2). Only those linear relationships with r -values < 0.7 (at 95% confidence level) were subjected to non-linear trend analysis. We are aware of the limitation due to statistically small number of samples ($n = 9$) and hence the documented relationships and interpretations need further refinements based on larger dataset.

Strong positive correlations between Mn and Fe and between Mn/Co and Fe/Co ($r = 0.84$ and 0.99 , respectively; table 2 and figure 3) contrast with generally observed inverse relationships in Pacific Fe–Mn crusts (Wen *et al* 1997 and references therein). Interestingly, Co is not correlated with Mn or Fe ($r < 0.2$; table 2 and figure 3), but shows a strong positive correlation with Ce ($r = 0.8$; table 2). These remarkable differences compared to Fe–Mn crusts studied elsewhere suggest that the compositional characteristics of the ANS Fe–Mn crusts are region specific (Rajani *et al* 2005).

Co concentrations vary inversely with water depth ($r = -0.78$; table 2 and figure 3A), whereas Ce and Ce/Co exhibit strong non-linear variations with water depth ($r = 0.86$ and 0.91 ; figure 4A and 4B), where trend reversal begins at ~ 2 km water depth. The linear inverse correlation of Co with water depth is well known (Halbach *et al* 1983), but the association of Ce and Ce/Co with water depth is opposite to that documented by Aplin (1984), who reported higher Ce contents in Fe–Mn crusts above 2000 m water depth in the Central Pacific. Our data can be interpreted to indicate (1) rapid removal of Ce to the Fe–Mn crusts in the upper ~ 2 km of the water column; (2) slower growth rates for crusts above ~ 2 km, or (3) a different source of Ce in the water mass below ~ 2 km. This approximately 2 km divide is clearly evident by a two-fold enrichment of Ce in samples above ~ 2 km water depth ($\sim 0.25\%$) compared to those below ($\sim 0.12\%$), irrespective of Fe and Mn contents (table 1).

